



# Synthesis of Methyl Lactate from Glycerol Using Sn-Beta Zeolite

Wenjie Dong, Chenlu Wang, Minyan Gu, Long Yang, Zheng Shen\* and Yalei Zhang\*

State Key Laboratory of Pollution Control and Resources Reuse, National Engineering Research Center of Facilities Agriculture, Key Laboratory of Yangtze River Water Environment of Ministry of Education, College of Environmental Science and Engineering, Tongji University, Shanghai 200092, China

Received October 14, 2016; Accepted March 6, 2017

**ABSTRACT:** Lactic acid can not only be used to produce multiple chemicals, but can also be the building block for biodegradable and biocompatible polylactic acid identified as a renewable resource. As a by-product in biodiesel production, the glycerol yield increases with a rapid expansion of biodiesel. However, in the chemical and environmental fields it is still a great challenge to produce lactic acid or methyl lactate from glycerol. Herein, Sn-Beta zeolite was prepared through solid-state ion exchange (Sn-Beta SSIE) and was tested for base-free one-pot catalytic selective oxidation of glycerol into methyl lactate in methanol. The results showed that a maximum selectivity of up to 56.7% was achieved with a 36.8% conversion rate at 433 K within 4 h under an initial oxygen pressure of 0.1 MPa. In addition, the methyl lactate yield is not high because of its decomposition in the presence of oxygen. This study aims to contribute to the development of the polylactic acid industry.

**KEYWORDS:** Methyl lactate, glycerol, Sn-Beta zeolite, selective catalytic oxidation, heterogeneous catalyst

## 1 INTRODUCTION

The fast development of renewable polylactic acid has greatly increased the demand for quantities of lactic acid (LA), as it offers an alternative to fossil resources and benefits the environment [1, 2]. Currently, the main route to produce LA is the biological fermentation of carbohydrates, which has many disadvantages such as complex downstream processing, low efficiency and high cost [3]. To solve these problems, an ideal choice is to produce lactic acid or methyl lactate (ML) by utilizing biomass or wastes through a one-pot chemical method [4–6].

Sn-Beta zeolite is one of the favorable catalysts, which shows highly catalytic activity in many reactions, especially isomerization [7–9]. Taarning *et al.* first reported the conversion of dioxoacetone (DHA) and glyceraldehyde (GLA) into LA (90% selectivity) or ML (99% selectivity) using Sn-Beta zeolite obtained by hydrothermal synthesis [7]. His group further

developed catalytic processes for the direct formation of LA or ML using Sn-Beta zeolite from pentoses (xylose and arabinose), hexoses (glucose, fructose, galactose and mannose) and sucrose [4, 9]. As a heterogeneous catalyst, Sn-Beta zeolite can be repeatedly used and is easily separated compared with a homogeneous one; however, it is limited for large-scale application because of the complicated process and longer crystallization times, as well as the risk of environmental damage from using HF in the conventional hydrothermal method. The method of solid-state ion-exchange synthesis (SSIE) solves these problems well, and obtains a high-metal-content material [10]. Other synthesis methods [11–14] were also developed and they are very helpful for obtaining the optimal high activity Sn-Beta zeolite used in biomass conversion technology.

For the application of Sn-Beta zeolite in biomass conversion, the feedstock has at least an aldehyde or ketone group as an active group during the reaction. The catalytic conversion of a sugar alcohol, such as glycerol, over Sn-Beta zeolite is not addressed. Glycerol has become more available for multiplying in quantity with the rapid expansion of biodiesel [15]. Therefore, a project about the catalyzed transformations of glycerol

\*Corresponding authors: 78shenzheng@tongji.edu.cn; zhangyalei@tongji.edu.cn

DOI: 10.7569/JRM.2017.634126



into LA or ML would be significant. The production of LA from glycerol has also been reported using various chemical methods, including hydrogenolysis [16, 17], hydrothermal conversion [18, 19], and catalytic selective oxidation [20–23]. Cho *et al.* showed a base-free one-step reaction pathway to produce LA from the oxidation of glycerol over a Pt/Sn-MFI catalyst under milder conditions [24]. Purushothaman *et al.* reported the one-pot conversion of glycerol to ML using Au nanoparticles on zeolite-Y [25]. Sun *et al.* developed Iridium coordination polymers, which showed high catalytic activity and recyclability on the conversion of glycerol to potassium lactate [26]. More recently, their findings are valuable both in reality and in the academic field. However, noble metals were unavoidably used in their reaction systems.

In this article, the purpose of this study was to produce ML from glycerol over Sn-Beta SSIE and evaluate the effects of the operating conditions (e.g., catalyst dosage, oxygen pressure, temperature and reaction time) for achieving ML with high yield and selectivity. Meanwhile, the characteristics of Sn-Beta SSIE were revealed by XRD, TEM, XPS, FTIR and  $N_2$  adsorption.

## 2 EXPERIMENTAL

### 2.1 Catalyst Preparation

A commercial Beta zeolite (Beta) was purchased from the Catalyst Plant of Nankai University with a Si/Al ratio of 25. After the Beta zeolite was dealuminated by treatment in a  $HNO_3$  solution (65%, w/w) at 353 K for 20 h, the mixture was rinsed with water, isolated by centrifugal filtration several times until the supernatant was neutralized, and then dried at 423 K overnight. The deAl-Beta zeolite was used as seeds or parents for the formation of desired catalysts.

Sn-Beta SSIE was synthesized by grinding the deAl-Beta zeolite and tin(II) acetate [10]. The deAl-Beta zeolite was mixed with tin(II) acetate (200 mg per g) and ground for 30 min. The product was calcined under air flow at 823 K with a ramp of 2 K/min for 6 h. Following every run, the mixture was centrifuged to deposit the solid catalyst. The sample was calcined at 823 K for 6 h in static air to recover the catalyst.

Sn-Beta HT was synthesized by a classic hydrothermal method [4] using the following procedures: tetraethyl orthosilicate (TEOS) was added to a tetraethylammonium hydroxide solution (TEAOH) with stirring for approximately 90 minutes. An aqueous solution of tin(IV) chloride pentahydrate was then added to the prepared clear solution. The mixture was stirred until the ethanol that formed upon hydrolysis of TEOS was completely evaporated. The HF was

added to the resulting clear solution, and a thick gel was formed. The deAl-Beta seeds (4 wt% with respect to the theoretical zeolite amount) were suspended in deionized water, sonicated and dispersed in the gel. The composition of the final gel was  $SiO_2:0.008SnO_2:0.54TEAOH:0.54HF:11H_2O$ . The gel was transferred to a Teflon vessel in a stainless steel autoclave and crystallized at 413 K with a rotation of 20 rpm for 17 days. After crystallization, the product was rinsed with water, isolated by centrifugal filtration several times and dried at 383 K overnight. The dried zeolite was finally calcined in static air at 823 K with a ramp of 2 K/min for 10 h.

Sn-Beta WI was obtained by a wet impregnation method [12] with a tin(IV) chloride pentahydrate solution in isopropanol. The deAl-Beta zeolite was suspended in isopropanol (100 mL per g), and tin(IV) chloride pentahydrate (38 mmol per g) was added. The solution was refluxed under  $N_2$  for 7 h and afterwards rinsed with isopropanol. Then, the solution was isolated by centrifugal filtration and dried at 333 K overnight. The sample was calcined in static air at 473 K with a ramp of 2 K/min for 6 h and at 823 K for 6 h with the same heating rate.

### 2.2 Catalyst Characterization

The XRD data were recorded by a Bruker D8 Advance Powder X-ray Diffractometer (XRD, Germany) using a  $Cu K\alpha$  ( $\lambda = 1.54178 \text{ \AA}$ ) radiation source, while the operation voltage and current were kept at 40 kV and 40 mA, respectively. The morphologies of the zeolites were characterized using high-resolution TEM (Hitachi S-3000N) fitted with a Gatan TV camera. The Sn content in the catalysts was determined by inductively coupled plasma optical emission spectroscopy (ICP-OES, PerkinElmer Optima 2100 DV). Prior to the measurements, the catalysts were digested in an acidic mixture (HCl- $HNO_3$ -HF) at 343 K for 12 h.

Nitrogen adsorption/desorption isotherm measurements were performed using a Micromeritics ASAP 2020 instrument at 77 K. The samples were degassed under nitrogen flow at 573 K overnight prior to the measurement. The specific surface areas and micropore volumes were calculated by applying the BET and t-plot methods, respectively.

The photoemission spectra were measured using an Escalab 250Xi spectrometer (Thermo Scientific) with a monochromatized Al  $K\alpha$  X-ray source. The analyzer pass energy was 30 eV and the energy step was 0.05 eV. A binding energy of 284.8 eV for C1s was used as internal standard.

The acidic properties of catalysts were studied by adsorption and temperature programmed

desorption (TPD) of pyridine by Fourier transform infrared (FTIR) spectroscopy. The infrared spectra were recorded on a PerkinElmer Frontier FTIR spectrometer with a spectral resolution in the 1400–1700  $\text{cm}^{-1}$  range with a resolution of 2  $\text{cm}^{-1}$ . A 10 mg sample was pressed into a self-supported wafer with a diameter of 13 mm. The wafer was set in a quartz IR cell which was sealed with  $\text{CaF}_2$  windows and connected to a vacuum system. The samples were dried at 723 K for 2 h under vacuum. After cooling to room temperature, pyridine vapor was admitted into the cell and adsorption lasted for 0.5 h. Subsequently, desorption steps at 423 K (1 h) and 523 K (1 h) were performed.

### 2.3 Catalytic Reaction and Product Analysis

The reaction was investigated using a closed Teflon vessel in a stainless steel autoclave (Figure S1). A typical procedure for reaction was: 2.5 mmol glycerol, 8 g methanol as a solvent and a certain amount of catalyst were placed into a 100 mL autoclave. After the introduction of oxygen at a desired pressure, the reactor contents were heated to a desired temperature and kept for a desired time under stirring using a magnetic stir bar (700 rpm). Zero MPa of oxygen pressure in the test means an ambient nitrogen pressure. A continuous supplied oxygen experiment was carried out as follows: glycerol (2.50 mmol), methanol (8 g) and catalyst Sn-Beta SSIE (30 mg) were added into the reactor and pressured with 0.1 MPa of oxygen, gas source was cut off, the reactor was heated to 433 K (2.0 MPa in the autoclave as the temperature was reached) under stirring (700 rpm), the oxygen source valve (2.0 MPa) was turned on again to maintain balance with the internal pressure in the reactor, and 4 h of reaction time was applied. After the reaction, reaction samples were analyzed by gas chromatography (GC) using an Agilent 7820A instrument equipped with a DB-WAXetr capillary column (30.0 m  $\times$  320  $\mu\text{m}$   $\times$  0.25  $\mu\text{m}$ ) and an FID detector. An Agilent 7890A GC system coupled with an Agilent 5975C mass detector was used for qualitative

analysis.  $^1\text{H}$  NMR analyses were performed in  $\text{D}_2\text{O}$  on a Bruker DMX 400 spectrometer.

The glycerol conversion (%), ML yield and selectivity (%) were calculated using the following equations: glycerol conversion (%) = (moles of glycerol reacted/moles of glycerol taken)  $\times$  100%; ML yield (%) = (moles of ML obtained/moles of glycerol taken)  $\times$  100%; and ML selectivity (%) = (ML yield/ glycerol conversion)  $\times$  100%.

## 3 RESULTS AND DISCUSSION

### 3.1 Catalyst Characterization

Table 1 summarizes the physicochemical properties of the Beta-type zeolites. All samples exhibited similar BET surface areas (474–481  $\text{m}^2\text{g}^{-1}$ ) and pore volumes (0.19–0.20  $\text{cm}^3\text{g}^{-1}$ ), which were consistent with other reports in the literature [12, 27]. The Sn contents of Sn-Beta SSIE measured by ICP-OES were approximately 10.02%. This result indicates that sufficient Sn could be introduced into the Beta zeolite through the SSIE method. However, the contents of Sn in the Sn-Beta zeolites prepared through the HT and WI methods are limited. Because too much Sn will destroy the formation of the crystal structure of Beta zeolite in the HT method, and will block the molecular sieve pore in the WI method.

The microporous structure can be confirmed by the nitrogen adsorption/desorption isotherm measurements of the Beta-type zeolites (Figure S2). All of the isotherms presented were typical of microporous materials (type I) with a narrow hysteresis loop located at  $0.5 < P/P_0 < 0.8$ , suggesting the presence of mesopores in the structure [28]. A few mesoscopic pores around 3.69 nm were found from the pore size distribution of the desorption branch using the BJH method.

The XRD data of Beta-type zeolites and  $\text{SnO}_2$  were collected (Figure 1). From the patterns, it could be seen that similar XRD patterns to deAl-Beta and Beta were observed, indicating that the structure of the Beta zeolite is not destroyed during the process of  $\text{HNO}_3$  treatment.

**Table 1** Physicochemical properties of Beta, deAl-Beta and Sn-Beta SSIE.

Catalyst	BET <sup>a</sup> ( $\text{m}^2\text{g}^{-1}$ )	$V_{\text{micro}}^b$ ( $\text{cm}^3\text{g}^{-1}$ )	Sn <sup>c</sup> (wt%)	B <sup>d</sup> ( $\text{mmolg}^{-1}$ )		L <sup>d</sup> ( $\text{mmolg}^{-1}$ )	
				423 K	523 K	423 K	523 K
Beta	481.28	0.19	–	0.17	0.17	0.15	0.13
deAl-Beta	484.59	0.20	–	0	0	0	0
Sn-Beta SSIE	474.31	0.19	10.02	0.02	0	0.14	0.08

<sup>a</sup>Brunauer-Emmet-Teller surface area calculated by  $\text{N}_2$  physisorption; <sup>b</sup>Determined using the t-plot method; <sup>c</sup>Determined by ICP-OES analysis; <sup>d</sup>The number of Brønsted acid and Lewis acid sites based on pyridine IR adsorption.

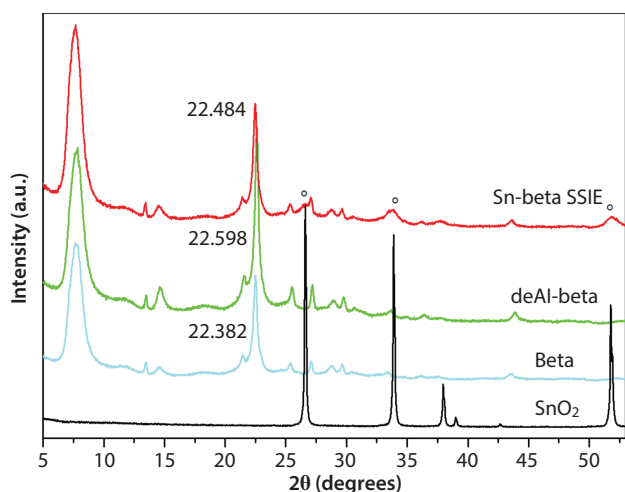


**Figure 1** XRD diffractograms of  $\text{SnO}_2$ , Beta, deAl-Beta and Sn-Beta SSIE.

The XRD pattern of the Sn-Beta SSIE displayed not only the characteristic diffraction peaks of the BEA topology, but also weak peaks of  $\text{SnO}_2$  (marked with a hollow circle in Figure 1). This phenomenon shows that very small amounts of crystalline  $\text{SnO}_2$  have been formed during the preparation of this sample owing to the high dosing of tin(II) acetate [29]. However, a successful incorporation of metal into the framework of deAl-Beta zeolite can be demonstrated through a matrix contraction/expansion of zeolite structure in the position of the diffraction peak (302) at  $2\theta = 22.5\text{--}22.6^\circ$  [30, 31]. The  $d_{302}$  spacing decreased from 3.968 (Beta,  $2\theta = 22.382^\circ$ ) to 3.931 Å (deAl-Beta,  $2\theta = 22.598^\circ$ ), suggesting a matrix contraction ascribed to the dealumination process. The slight increase of the  $d_{302}$  spacing from 3.931 (deAl-Beta,  $2\theta = 22.598^\circ$ ) to 3.951 Å (Sn-Beta SSIE,  $2\theta = 22.484^\circ$ ) showed a matrix expansion of zeolite structure after the introduction of Sn.

The TEM images of the Beta-type zeolites show that there are no obvious alterations of the crystalline structure for the deAl-Beta and Sn-Beta SSIE compared with rude Beta (Figure S3). In the case of Sn-Beta SSIE, it might be  $\text{SnO}_2$ , which is finely dispersed, and the particles were uniform tiny spheres with a size of approximately 5–10 nm. This result is consistent with XRD data, but the presence of extra-framework Sn will lead to reduced activity for ML formation [4]. An XPS experiment was carried out to analyze the state of Sn. The results indicate that the framework tin could be confirmed by Sn 3d signals located at 487.1 eV and 495.5 eV in the Sn-Beta SSIE (Figure S4), which were different from the extra-framework Sn 3d signals of  $\text{SnO}_2$  located at 486.1 eV and 494.5 eV [32].

In general, our results show that some of the tin atoms are incorporated into the framework through

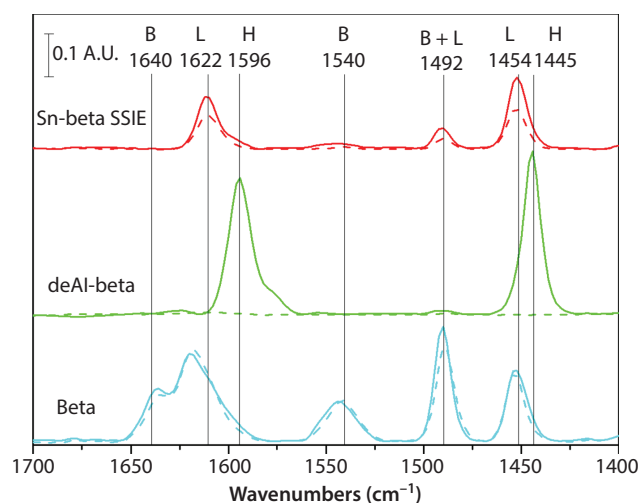


**Figure 2** FTIR spectra of pyridine adsorbed at 150 °C (solid line) and 250 °C (dotted line) of Beta, deAl-Beta and Sn-Beta SSIE.

the SSIE method from the XRD and XPS patterns. And some of the tin atoms are not incorporated into the framework and might exist in the form of  $\text{SnO}_2$ , which could be verified by the XRD pattern and TEM.

The catalyst surface acid sites are an important factor for the catalytic conversion to produce LA or ML [4, 8, 33, 34]. FTIR spectroscopy was used to analyze the surface acid site of catalysts after pyridine chemisorptions at 150 °C and 250 °C (Figure 2). The characteristic absorbed peaks in the FTIR spectra represent the presence of Lewis acid sites (1454, 1492, 1622  $\text{cm}^{-1}$ ), Brønsted acid sites (1492, 1540, 1640  $\text{cm}^{-1}$ ) and hydroxyl groups (1445, 1596  $\text{cm}^{-1}$ ) [35]. In the case of Beta zeolite, both Lewis and Brønsted acid sites existed. Following  $\text{HNO}_3$  treatment, they were completely removed from the FTIR spectra, indicating the complete removal of framework Al. However, two extra new bands appeared at 1445 and 1596  $\text{cm}^{-1}$  representing hydroxyl groups by the formation of pyridine and the surface silanol groups [35, 36], and they disappeared when the desorption temperature was increased to 250 °C. In the case of Sn-Beta SSIE, the introduction of Sn gave rise to Lewis acid sites again in the catalysts. The characteristics of a small amount of Brønsted acidity and very weak Lewis acidity in the Sn-Beta SSIE, which decreased from 0.014 to 0.08  $\text{mmol g}^{-1}$  as the temperature increased from 423 to 523 K, might match the requirements for an ideal catalyst to produce ML, but not a large amount of strong Brønsted and Lewis acidity (Table 1). In addition, hydroxyl groups were not found in the Sn-Beta SSIE, which is further evidence that Sn had been incorporated into the framework by replacing the sites of hydroxyl groups in the deAl-Beta.



## 3.2 Conversion of Glycerol into Methyl Lactate

### 3.2.1 Influence of Catalysts

To verify the role of Sn-Beta SSIE in the conversion of glycerol into ML, the catalytic efficiency of the Beta-type zeolites was evaluated. As shown in Table 2, the conversion of glycerol was improved to 72.1% from 39.1% by dosing Beta instead of deAl-Beta, but their yields of ML were neglected (entries 1 and 2). The above results show that the strong Brønsted and Lewis acidity of Beta zeolite could accelerate the conversion of glycerol, but has poor ability to generate ML.

Sn-Beta zeolites were synthesized through three methods, including hydrothermal synthesis, wet impregnation and SSIE. In the experiments, the moles of Sn were controlled at the same level by the catalyst dosage. After introducing Sn, the conversion of glycerol and the yield of ML were significantly improved compared to the deAl-Beta zeolite as a catalyst (entries 3–5). This could be explained by the fact that the Lewis acid ascribed to the introduction of Sn plays an important role in the selectivity and catalytic conversion [4]. Considering the easy preparation (short time consumption, easy handling), environmental protection (HF and structure-directing agents were avoided), possibility of large-scale applicability (more active metal incorporated into the zeolite) and comparable catalytic efficiency, Sn-Beta SSIE was selected to study in the following experiments. Importantly, it was confirmed that the least dosage of Sn-Beta SSIE had been used and that this catalyst could be reused as its stable structure (entry 6). In addition, SnO<sub>2</sub> showed a poor catalytic efficiency in this test (entry 7), indicating that the framework for tin incorporation is a critical factor to obtain an efficient catalyst.

### 3.2.2 Influence of Dosage

The effect of the catalyst amount was investigated by varying the catalyst mass in the range of 7.5 to 90 mg.

The glycerol conversion rapidly increased with the increase of the catalyst amount up to 30 mg; thereafter, the conversion remained unchanged (approximately 80%) (Figure S5). Obviously, more catalyst dosages provide more active sites for glycerol conversion; however, the maximum conversion of glycerol (78.0%) was achieved when 30 mg of catalyst was used. Meanwhile, the influence of the ML yield is not significant with an increase of Sn-Beta SSIE.

### 3.2.3 Influence of Oxygen Pressure

The effect of the oxygen pressure was studied by varying this parameter in the range of 0 to 0.6 MPa, and the results are shown in Figure 3. It should be noted that glycerol would not be converted without oxygen in this system. The conversion of glycerol was increased from 36.8% at an oxygen pressure of 0.1 MPa to 78.0% at an oxygen pressure of 0.6 MPa. In contrast, the selectivity for ML clearly dropped from 56.7% to 19.3%. A higher oxygen pressure has a positive effect on the glycerol

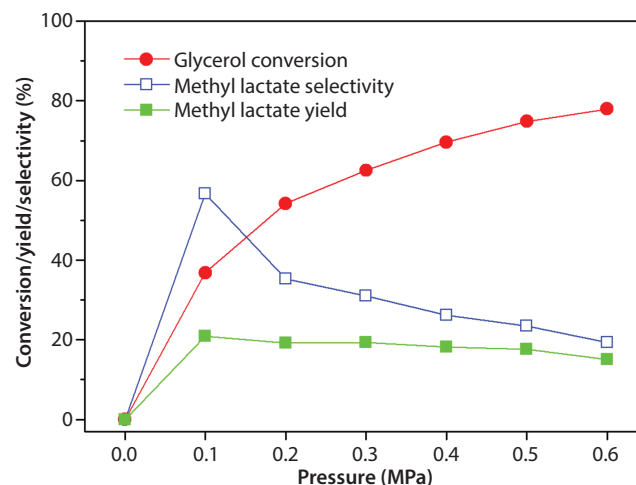


**Figure 3** Effect of the oxygen pressure on the selective oxidation of glycerol over Sn-Beta SSIE (glycerol [2.50 mmol], methanol [8 g], catalyst [30 mg], 433 K, 4 h).

**Table 2** Selective oxidation of glycerol over different catalysts.<sup>a</sup>

Entry	Catalyst	Dosage (mg)	Conversion (%)	Yield (%)	Selectivity (%)
1	Beta	160	72.1	4.7	6.5
2	deAl-Beta	160	39.1	2.9	7.3
3	Sn-Beta HT	160	79.5	11.7	14.7
4	Sn-Beta WI	420	71.7	14.7	20.2
5	Sn-Beta SSIE	14	69.4	14.0	20.1
6 <sup>b</sup>	Sn-Beta SSIE	14	67.5	12.4	18.3
7	SnO <sub>2</sub>	2	31.8	2.9	9.2

<sup>a</sup>Reaction conditions: glycerol (2.50 mmol), methanol (8 g),  $p_{O_2}$  = 0.6 MPa, 433 K, 4 h. <sup>b</sup>Third use of the catalyst.

conversion but is not beneficial for ML formation. The maximum yield of ML over Sn-Beta SSIE was only 20.9% at a lower initial oxygen pressure (0.1 MPa), and the corresponding selectivity reached 56.7%. From the above results, it could be suggested that the initial oxygen pressure is one of the key parameters during the process of selective conversion of glycerol into ML in methanol.

Considering that the largest ML yield was achieved with a lower glycerol conversion (36.8%), we presumed that a higher oxygen pressure was harmful to ML selectivity, and at the same time, oxygen was insufficient to oxidize glycerol at 0.1 MPa. Based on these presumptions, a continuously supplied low pressure of oxygen experiment was carried out. In this continuous oxygen supply experiment, the glycerol conversion increased to 67.7%; however, the ML selectivity decreased to 23.1%. This result demonstrates that oxygen is consumed in the process of glycerol oxidation. Surplus oxygen supplied at a low and constant pressure also had an adverse effect on producing ML. Similar results (65.5% conversion and 22.5% selectivity) could be obtained with air as a safer and cheaper gas source instead of oxygen. The initial air pressure (0.5 MPa in this work) should be higher compared with oxygen as the gas source in order to obtain comparable oxygen content.

### 3.2.4 Influence of Reaction Temperature and Time

The data in Table 3 present the effects of the reaction temperature and reaction time. After 4 h at 373 K, no reaction occurred (entry 1). When the reaction temperature was increased from 403 to 453 K, the glycerol conversion increased from 54.0% to 89.1%; however, the ML yield only increased from 12.0% to 14.6%. This result suggests that the temperature has an obvious effect on the glycerol oxidation but a slight positive effect on the ML yield under these conditions. Entries

3 to 7 show the influence of reaction time by varying this parameter in the range of 2 to 20 h. It was found that both the glycerol conversion and ML selectivity remained relatively stable after the time exceeded 4 h. Due to the weaker effect of time on the reaction, a longer reaction time was not adopted in this study.

### 3.3 Reason for Low ML Yield

In the published works [24, 37], the conversion of glycerol into ML involved the oxidative dehydrogenation of glycerol to dioxyacetone (DHA) or glyceraldehyde and the subsequent catalyzed dehydration to pyruvaldehyde followed by the formation of ML in the presence of a Lewis acid catalyst. Here, we studied the reactive behavior of DHA under the following reaction conditions: DHA (2.50 mmol), methanol (8 g), Sn-Beta SSIE catalyst (30 mg),  $p_{O_2} = 0-1.0$  MPa, 433 K, and 4 h. As revealed in Figure 4, at an oxygen pressure

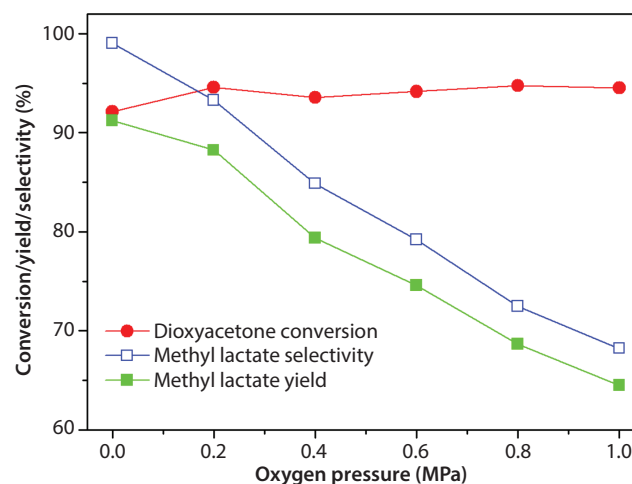


**Figure 4** Effect of the oxygen pressure on the catalytic oxidation of DHA over Sn-Beta SSIE (DHA [2.50 mmol], methanol [8 g], catalyst [30 mg], 433 K, 4 h).

**Table 3** Effect of the reaction temperature and time on the selective oxidation of glycerol over Sn-Beta SSIE.<sup>a</sup>

Entry	Temperature (K)	Time (h)	Conversion (%)	Yield (%)	Selectivity (%)
1	373	4	0	0	–
2	403	4	54.0	12.0	22.2
3	433	2	73.1	12.9	16.4
4	433	4	77.9	14.9	19.3
5	433	8	79.6	15.0	18.8
6	433	16	82.2	15.8	18.0
7	433	20	83.5	14.4	17.3
8	453	4	89.1	14.6	16.4

<sup>a</sup>Reaction conditions: glycerol (2.50 mmol), methanol (8 g), catalyst (30 mg),  $p_{O_2} = 0.6$  MPa.

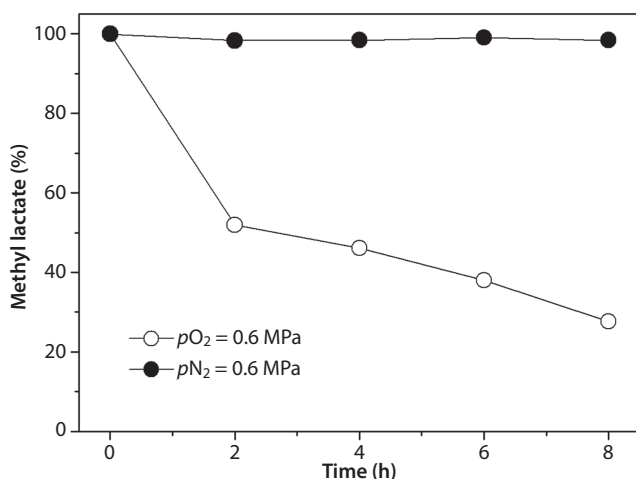


**Figure 5** Stability of methyl lactate over Sn-Beta SSIE (methyl lactate [2.50 mmol], methanol [8 g], catalyst [30 mg],  $p_{O_2} = 0.6$  MPa or  $p_{N_2} = 0.6$  MPa, 433 K).

of 0 MPa, the DHA conversion reached 92.1%, and the corresponding ML selectivity achieved was 99.0% over Sn-Beta SSIE. The good performance of Sn-Beta SSIE on isomerization of DHA was comparable to that of other reports using Sn-Beta HT [28, 38]. However, with an increase in the oxygen pressure, the yield of ML sharply declined, dropping to 64.5% at 1.0 MPa of oxygen pressure. Furthermore, methyl pyruvate and methyl glycolate were detected in the products. It has been reported that pyruvic acid could be produced from the oxidation of LA [24]. Therefore, we suggested that the further oxidation of ML might be a key reason for the low yield.

To confirm the degradation of ML, a series of stability studies were carried out under the following reaction conditions: ML (2.5 mmol), methanol (8 g), Sn-Beta SSIE catalyst (30 mg),  $p_{O_2}$  or  $p_{N_2} = 0.6$  MPa, and 433 K. In the presence of oxygen, the conversion of ML was 48.1% after 2 h and increased to 72.4% after 8 h (Figure 5). On the contrary, in the presence of nitrogen, ML remained unreacted. Hence, the degradation of ML actually occurs, which is different from previous reports [24, 25]. In comparison with gas chromatograms of products from glycerol and methyl lactate as the initial substance (Figure S6), it could be seen that methyl formate, methyl pyruvate and methyl glycolate (the other peaks were unidentified) were identified concurrently, which further demonstrates that these by-products were derived from the further oxidation of ML (Figure S7). The  $^1\text{H-NMR}$  spectra for the sample obtained after the conversion of glycerol are shown in Figure S8. The result confirmed the formation of methyl lactate and other unknown organic compounds. All in all, oxygen is a prerequisite for the oxidation of glycerol, as previously mentioned; while

excessive oxygen in this reaction system causes the decomposition of ML. Therefore, a weaker oxidant might be used to replace oxygen for this catalytic process, and further studies would be necessary.

## 4 CONCLUSIONS

Sn-Beta zeolite prepared by SSIE was applied for base-free one-pot catalytic conversion of glycerol into ML in methanol. In the catalytic experiments, the maximum selectivity of ML was up to 56.7%, and the corresponding conversion of glycerol was 36.8% over Sn-Beta SSIE under optimal reaction conditions. The decomposition of ML was a key reason for the low yield in this reaction system. In the Sn-Beta SSIE, parts of Sn atoms are incorporated into the framework of zeolite, as demonstrated by XRD, XPS and FTIR patterns, and others exist in the form of  $\text{SnO}_2$ , which were verified by the XRD pattern and TEM. This study has contributed to finding an effective catalyst to produce ML so as to promote the development of the renewable polylactic acid industry.

## ACKNOWLEDGMENTS

This work was supported by the National Science Fund for Distinguished Young Scholars (51625804), the National Natural Science Foundation of China (21376180, 21676205), the Fundamental Research Funds for the Central Universities (2870219026, 2870219028) and the International Collaborative Project from the Shanghai Science and Technology Commission (14230710800).

## REFERENCES

1. M. Dusselier, P. Van Wouwe, A. Dewaele, E. Makshina, and B.F. Sels, Lactic acid as a platform chemical in the biobased economy: The role of chemocatalysis. *Energy Environ. Sci.* **6**, 1415–1442 (2013).
2. D. Grewell, G. Srinivasan, and E. Cochran, Depolymerization of post-consumer polylactic acid products. *J. Renew. Mater.* **2**, 157–165 (2014).
3. Y. Wang, Y. Tashiro, and K. Sonomoto, Fermentative production of lactic acid from renewable materials: Recent achievements, prospects, and limits. *J. Biosci. Bioeng.* **119**, 10–18 (2015).
4. M.S. Holm, S. Saravanamurugan, and E. Taarning, Conversion of sugars to lactic acid derivatives using heterogeneous zeolite catalysts. *Science* **328**, 602–605 (2010).
5. W. Dong, Z. Shen, B. Peng, M. Gu, X. Zhou, B. Xiang, and Y. Zhang, Selective chemical conversion of sugars in aqueous solutions without alkali to lactic acid over a Zn-Sn-Beta Lewis acid-base catalyst. *Sci. Rep.* **6**, 26713 (2016).

6. M. Dusselier, R. De Clercq, R. Cornelis, and B.F. Sels, Tin triflate-catalyzed conversion of cellulose to valuable ( $\alpha$ -hydroxy-) esters. *Catal. Today* **279**, 339–344 (2017).
7. E. Taarning, S. Saravanamurugan, M. Spangsborg Holm, J. Xiong, R.M. West, and C.H. Christensen, Zeolite-catalyzed isomerization of triose sugars. *ChemSusChem* **2**, 625–627 (2009).
8. R. Bermejo-Deval, R.S. Assary, E. Nikolla, M. Moliner, Y. Román-Leshkov, S.-J. Hwang, A. Palsdottir, D. Silverman, R.F. Lobo, and L.A. Curtiss, Metalloenzyme-like catalyzed isomerizations of sugars by Lewis acid zeolites. *P. Natl. Acad. Sci.* **109**, 9727–9732 (2012).
9. M.S. Holm, Y.J. Pagán-Torres, S. Saravanamurugan, A. Riisager, J.A. Dumesic, and E. Taarning, Sn-Beta catalyzed conversion of hemicellulosic sugars. *Green Chem.* **14**, 702–706 (2012).
10. C. Hammond, S. Conrad, and I. Hermans, Simple and Scalable preparation of highly active lewis acidic Sn- $\beta$ . *Angew. Chem. Int. Ed.* **51**, 11736–11739 (2012).
11. P. Li, G. Liu, H. Wu, Y. Liu, J. Jiang, and P. Wu, Postsynthesis and selective oxidation properties of nanosized Sn-beta zeolite. *J. Phys. Chem. C* **115**, 3663–3670 (2011).
12. J. Dijkmans, D. Gabriëls, M. Dusselier, F. de Clippel, P. Vanelderden, K. Houthoofd, A. Malfliet, Y. Pontikes, and B.F. Sels, Productive sugar isomerization with highly active Sn in dealuminated  $\beta$  zeolites. *Green Chem.* **15**, 2777–2785 (2013).
13. Z. Kang, X. Zhang, H. Liu, J. Qiu, and K. L. Yeung, A rapid synthesis route for Sn-Beta zeolites by steam-assisted conversion and their catalytic performance in Baeyer-Villiger oxidation. *Chem. Eng. J.* **218**, 425–432 (2013).
14. P.Y. Dapsens, C. Mondelli and J. Pérez-Ramírez, Alkaline-assisted stannation of beta zeolite as a scalable route to Lewis-acid catalysts for the valorisation of renewables. *New J. Chem.* **40**, 4136–4139 (2016).
15. F.I. Altuna, B. Fernández-d'arlas, M. Corcuera, A. Eceiza, M.I. Aranguren, and P.M. Stefani, Synthesis and characterization of polyurethane rigid foams from soybean oil-based polyol and glycerol. *J. Renew. Mater.* **4**, 275–284 (2016).
16. E.P. Maris, W.C. Ketchie, M. Murayama, and R.J. Davis, Glycerol hydrogenolysis on carbon-supported PtRu and AuRu bimetallic catalysts. *J. Catal.* **251**, 281–294 (2007).
17. S. Zhu, J. Wang, and W. Fan, Graphene-based catalysis for biomass conversion. *Catal. Sci. Technol.* **5**, 3845–3858 (2015).
18. Z. Shen, F. Jin, Y. Zhang, B. Wu, A. Kishita, K. Tohji, and H. Kishida, Effect of alkaline catalysts on hydrothermal conversion of glycerin into lactic acid. *Ind. Eng. Chem. Res.* **48**, 8920–8925 (2009).
19. Y. Zhang, Z. Shen, X. Zhou, M. Zhang, and F. Jin, Solvent isotope effect and mechanism for the production of hydrogen and lactic acid from glycerol under hydrothermal alkaline conditions. *Green Chem.* **14**, 3285–3288 (2012).
20. P. Lakshmanan, P.P. Upare, N.T. Le, Y.K. Hwang, D.W. Hwang, U. Lee, H.R. Kim, and J.S. Chang, Facile synthesis of CeO<sub>2</sub> supported gold nanoparticle catalysts for selective oxidation of glycerol into lactic acid. *Appl. Catal. A-Gen.* **468**, 260–268 (2013).
21. R.M. West, M.S. Holm, S. Saravanamurugan, J.M. Xiong, Z. Beversdorf, E. Taarning, and C.H. Christensen, Zeolite H-USY for the production of lactic acid and methyl lactate from C-3 sugars. *J. Catal.* **269**, 122–130 (2010).
22. G. Yang, Y. Ke, H. Ren, C. Liu, R. Yang, and W. Dong, The conversion of glycerol to lactic acid catalyzed by ZrO<sub>2</sub>-supported CuO catalysts. *Chem. Eng. J.* **283**, 759–767 (2016).
23. H. Yin, C. Zhang, H. Yin, D. Gao, L. Shen, and A. Wang, Hydrothermal conversion of glycerol to lactic acid catalyzed by Cu/hydroxyapatite, Cu/MgO, and Cu/ZrO<sub>2</sub> and reaction kinetics. *Chem. Eng. J.* **288**, 332–343 (2016).
24. H.J. Cho, C.C. Chang, and W. Fan, Base free, one-pot synthesis of lactic acid from glycerol using a bifunctional Pt/Sn-MFI catalyst. *Green Chem.* **16**, 3428–3433 (2014).
25. P. Purushothaman, R. Kumar, J. van Haveren, I. Melián-Cabrera, E.R. van Eck, and H.J. Heeres, Base-free, one-pot chemocatalytic conversion of glycerol to methyl lactate using supported gold catalysts. *ChemSusChem* **7**, 1140–1147 (2014).
26. Z. Sun, Y. Liu, J. Chen, C. Huang, and T. Tu, Robust iridium coordination polymers: Highly selective, efficient, and recyclable catalysts for oxidative conversion of glycerol to potassium lactate with dihydrogen liberation. *ACS Catal.* **5**, 6573–6578 (2015).
27. C.M. Osmundsen, M.S. Holm, S. Dahl, and E. Taarning, Tin-containing silicates: Structure-activity relations. *P. Roy. Soc. Lond. A. Mat.* **468**, 2000–2016 (2012).
28. C. Chang, Z. Wang, P. Dornath, H.J. Cho, and W. Fan, Rapid synthesis of Sn-Beta for the isomerization of cel-lulosic sugars. *RSC Adv.* **2**, 10475–10477 (2012).
29. P. Wolf, M. Valla, A.J. Rossini, A. Comas-Vives, F. Núñez-Zarur, B. Malaman, A. Lesage, L. Emsley, C. Copéret, and I. Hermans, NMR signatures of the active sites in Sn- $\beta$  zeolite. *Angew. Chem. Int. Ed.* **126**, 10343–10347 (2014).
30. R. Baran, F. Averseng, Y. Millot, T. Onfroy, S. Casale, and S. Dzwigaj, Incorporation of Mo into the vacant T-atom sites of the framework of BEA zeolite as mononuclear Mo evidenced by XRD and FTIR, NMR, EPR, and DR UV-Vis spectroscopies. *J. Phys. Chem. C* **118**, 4143–4150 (2014).
31. R. Baran, T. Onfroy, S. Casale, and S. Dzwigaj, Introduction of Co into the vacant T-atom sites of SiBEA zeolite as isolated mononuclear Co species. *J. Phys. Chem. C* **118**, 20445–20451 (2014).
32. H. Luo, L. Bui, W. Gunther, E. Min, and Y. Román Leshkov, Synthesis and catalytic activity of Sn-MFI nanosheets for the Baeyer-Villiger oxidation of cyclic ketones. *ACS Catal.* **2**, 2695–2699 (2012).
33. Q. Guo, F. Fan, E.A. Pidko, W.N.P. van der Graaff, Z. Feng, C. Li, and E.J.M. Hensen, Highly active and recyclable Sn-MWW zeolite catalyst for sugar conversion to methyl lactate and lactic acid. *ChemSusChem* **6**, 1352–1356 (2013).
34. P.Y. Dapsens, C. Mondelli, and J. Pérez-Ramírez, Highly selective lewis acid sites in desilicated MFI zeolites for dihydroxyacetone isomerization to lactic acid. *ChemSusChem* **6**, 831–839 (2013).



35. L. Li, C. Stroobants, K. Lin, P.A. Jacobs, B.F. Sels, and P.P. Pescarmona, Selective conversion of trioses to lactates over Lewis acid heterogeneous catalysts. *Green Chem.* **13**, 1175–1181 (2011).
36. T. Conesa, J. Hidalgo, R. Luque, J. Campelo, and A. Romero, Influence of the acid-base properties in Si-MCM-41 and B-MCM-41 mesoporous materials on the activity and selectivity of  $\epsilon$ -caprolactam synthesis. *Appl. Catal. A-Gen.* **299**, 224–234 (2006).
37. R.K.P. Purushothaman, J. van Haveren, D.S. van Es, I. Melián-Cabrera, J.D. Meeldijk, and H.J. Heeres, An efficient one pot conversion of glycerol to lactic acid using bimetallic gold-platinum catalysts on a nanocrystalline CeO<sub>2</sub> support. *Appl. Catal. B-Environ.* **147**, 92–100 (2014).
38. C.M. Lew, N. Rajabbeigi, and M. Tsapatsis, Tin-containing zeolite for the isomerization of cellulosic sugars. *Micropor. Mesopor. Mat.* **153**, 55–58 (2012).

### Supplementary Document Available Online

[http://www.scribenerpublishing.com/journalsuppl/jrm/JRM-2016-0070/jrm\\_JRM-2016-0070\\_supp1.docx](http://www.scribenerpublishing.com/journalsuppl/jrm/JRM-2016-0070/jrm_JRM-2016-0070_supp1.docx)